OH and CH continuous opacity in solar and stellar atmospheres

Kurucz, R.L.; Dishoeck, E.F. van; Tarafdar, S.P.

THE ASTROPHYSICAL JOURNAL, 322:992–998, 1987 November 15

OH AND CH CONTINUOUS OPACITY IN SOLAR AND STELLAR ATMOSPHERES

ROBERT L. KURUCZ AND EWINE F. VAN DISHOECK[1]
Harvard-Smithsonian Center for Astrophysics

AND

S. P. TARAFDAR
Tata Institute of Fundamental Research
Received 1987 March 27; accepted 1987 May 5

ABSTRACT

Continuous absorption cross sections of OH and CH have been computed for the temperature range 1000 K to 9000 K. Both OH and CH produce significant ultraviolet opacity in the Sun and cool stars. CH is also significant in the visible at 400 nm.

Subject headings: molecular processes — opacities — stars: atmospheres

I. INTRODUCTION

Our knowledge of the contributions to the opacity in stellar atmospheres is still incomplete. Tarafdar and Das (1975) and Fox and Tarafdar (1978) proposed that continuous absorptions from the ground state to repulsive upper states of OH and CH might produce significant opacity in the atmospheres of the Sun and later type stars at $\lambda > 250$ nm. However, as the absorption cross sections and excitation energies for the transitions were not known at that time, their results were based on very approximate molecular data. Recently, van Dishoeck and Dalgarno (1983, 1984) and van Dishoeck (1987) have performed accurate quantum chemical calculations of the excited electronic states of the OH and CH molecules and have presented photodissociation cross sections for use in the modeling of interstellar clouds. In this work, we extend these calculations to higher levels to provide a set of cross sections for use in model stellar atmospheres. In the final section, we estimate the effect of this source of ultraviolet opacity on the solar continuum.

II. OH AND CH CROSS SECTIONS

Continuous absorption from the ground $X^2\Pi$ state of OH can occur into the repulsive parts of the excited $1^2\Sigma^-$, $1^2\Delta$, $B^2\Sigma^+$, and coupled 2 and $3^2\Pi$ states. Potential energy curves for these states and the transition dipole moment functions connecting them have been calculated using *ab initio* self-consistent-field plus configuration-interaction quantum chemical methods by van Dishoeck, Langhoff, and Dalgarno (1983) and van Dishoeck and Dalgarno (1983), and absorption cross sections starting from the lowest vibrational level of the molecule have been reported. In this work, cross sections starting from all vibrational levels of the ground state are computed.

The vibrational wave functions for the ground $X^2\Pi$ state were evaluated using an empirical RKR potential based on the constants of Coxon and Forster (1982) up to $v = 10$, extended to longer and shorter internuclear distances by the theoretical potential obtained with basis set I by van Dishoeck, Langhoff, and Dalgarno (1983). The employed $1^2\Sigma^-$ and $B^2\Sigma^+$ potentials, as well as the $1^2\Sigma^-$–$X^2\Pi$ transition moment function, were taken from the same basis set I calculations. The $1^2\Delta$ potential curve, together with the $1^2\Delta$–$X^2\Pi$ and $B^2\Sigma^+$–$X^2\Pi$ transition moment functions, were taken from the Gaussian calculations of van Dishoeck and Dalgarno (1983). The absorption into the coupled $2^2\Pi$ and $3^2\Pi$ states has been treated in the diabatic approximation, in which continuous absorption occurs into the diabatic repulsive state (cf. van Dishoeck *et al.* 1984). The repulsive diabatic $^2\Pi$ potential, and the diabatic $^2\Pi$–$X^2\Pi$ transition moment function, were obtained from the Gaussian calculation of van Dishoeck *et al.* (1984).

Continuous absorption in CH takes place from its ground $X^2\Pi$ state into the excited $B^2\Sigma^-$, $2^2\Sigma^+$, and coupled 2, 3, and $4^2\Pi$ states. In addtion, CH has a low-lying $a^4\Sigma^-$ state only 0.7 eV above the ground $X^2\Pi$ state, which can be populated significantly at higher temperatures. Continuous absorption starting from the $a^4\Sigma^-$ state can occur into the upper $1^4\Pi$ and $2^4\Sigma^-$ states. All potential energy curves and transition dipole moment functions used in this work were taken from the calculations of van Dishoeck (1987). As for OH, the absorption into the coupled excited CH $^2\Pi$ states was computed using the diabatic approximation.

The method of calculation of the cross sections was the same as outlined by van Dishoeck and Dalgarno (1983), except that the centrifugal term $J(J+1)/2\mu R^2$, where J is the rotational quantum number, was retained in the solution of the radial nuclear eigenvalue equation. Computations were performed for all v with $J = 0$, 15, 25, 35, and 45 as long as the vibration-rotation level was bound. Figure 1 illustrates the variation of the OH cross sections with increasing J for absorption into the $1^2\Sigma^-$ state starting from the $X^2\Pi$ $v = 0$ level. The uncertainties in the magnitudes of the cross sections are estimated to be less than 25% in general, whereas the errors in the positions of the maxima are typically ± 0.2 eV (corresponding to ± 30 Å). The only exception is the cross section for absorption into the continuum of the CH $B^2\Sigma^-$ state at $\lambda < 360$ nm. Because the $B^2\Sigma^-$ potential has a small hump at larger internuclear distances, the calculations at photon energies just above threshold are extremely sensitive to the details of the $B^2\Sigma^-$ potential curve. As a result, the computed cross sections from the lowest levels of the $X^2\Pi$ state with $v < 2$, $J < 20$ are uncertain by up to a factor of 3.

Cross sections of OH and CH were calculated over a wide range of photon energies with a typical spacing of 0.05 eV. All computed cross sections were interpolated to the same 0.01 eV spacing. The LTE Boltzmann-averaged cross section per mol-

[1] Junior Fellow, Harvard Society of Fellows.

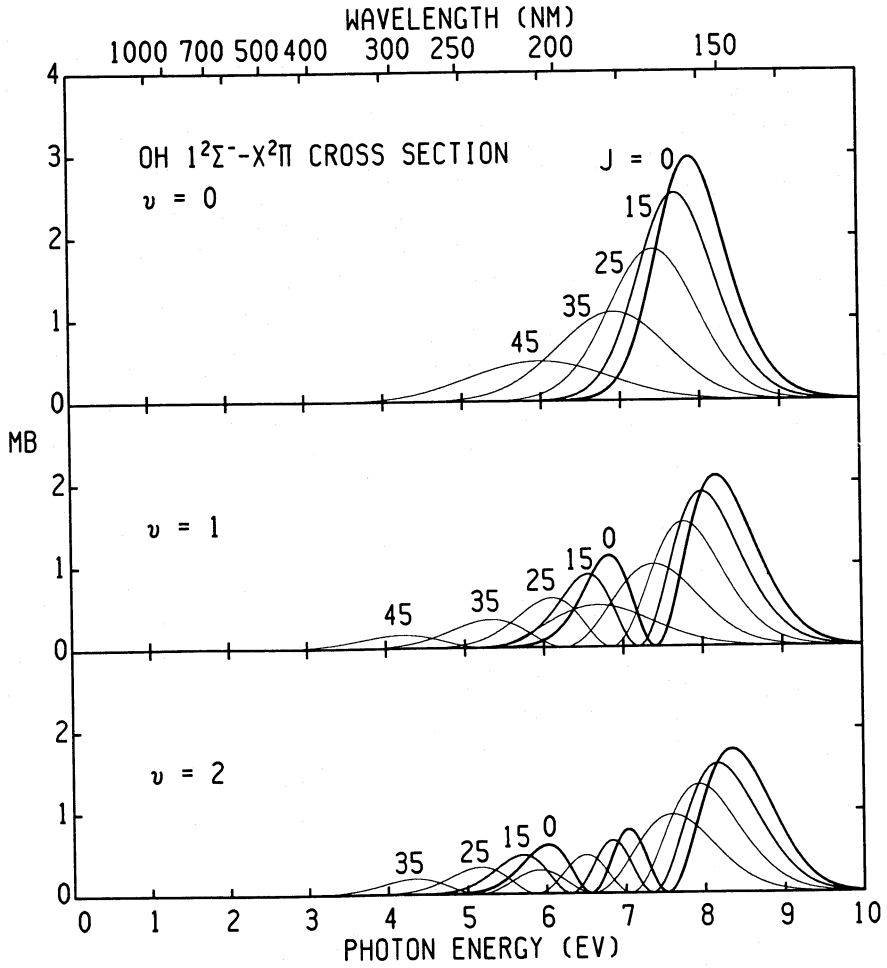

FIG. 1.—Computed cross sections for continuous absorption of OH from the $X^2\Pi(v, J)$ state into the $1^2\Sigma^-$ state for $v = 0$ (*top*), 1 (*middle*), 2 (*bottom*), and various rotational quantum numbers J.

ecule was computed as a function of temperature by direct summation over every bound energy level using either the cross section interpolated in J or that for the nearest J. The partition function was computed by summing over every bound level of all low-lying electronic states, X and A for OH, and X, a, A, B, and C for CH.

The LTE Boltzmann-averaged cross sections for OH and CH are presented in Tables 1 and 2. They are plotted as a function of energy and wavelength in Figures 2 and 3. The contribution of each electronic transition at a typical solar temperature of 5000 K is shown in Figures 4 and 5. At this temperature, about 61% of the OH molecules reside in $v = 0$, 18% in $v = 1$, and the remaining 21% in higher v. Within $v = 0$, the rotational distribution peaks around $J = 10$. The distribution of the CH molecules over the $X^2\Pi(v, J)$ levels is similar to that of OH, except that 13% of the molecules are in the $a^4\Sigma^-$ state. Because the majority of the OH and CH molecules reside in $v = 0$, the averaged cross sections are qualitatively "broadened" versions of the $v = 0$, $J = 0$ cross sections presented by van Dishoeck and Dalgarno (1983, 1984) and van Dishoeck (1987). Compared with the estimate of Tarafdar and Das (1975), the present OH cross sections for the $1^2\Sigma^-$ channel are a factor of 30 larger at peak around 170 nm, but fall off much more rapidly at longer wavelengths. The $B^2\Sigma^-$ cross section obtained in this work is similar in magnitude to that estimated by Tarafdar and Das (1975) but is shifted to longer wavelengths.

Computer readable cross sections for individual levels for use in non–LTE calculations or the complete tables can be obtained from Kurucz.

III. EFFECT ON SOLAR AND STELLAR CONTINUUM FLUXES

We estimated the effect of the CH and OH opacities on the solar continuum using Allen's LTE solar model (1978) in Kurucz's spectrum synthesis program (Kurucz and Avrett 1981) without including line absorptions. The result is shown in Figure 6. Below 150 nm, the continuum of the Sun is formed mostly in the chromosphere where the contribution of OH and CH is negligible. However, between 170 and 250 nm, the OH and CH opacities dramatically affect the ultraviolet continuum flux. OH contributes mostly to the opacity in the 170–190 nm region, with all other differences caused by CH. The actual contributions are somewhat uncertain, because the computed molecular abundances in the Sun are model-dependent and because all opacities may be affected by non–LTE conditions. Nevertheless, we can conclude that OH and CH have an effect on the solar continuum flux between 150 and 250 nm of the order of tens of percent. CH may also contribute on the order of several percent around 400 nm, where absorption into the low-lying $B^2\Sigma^-$ state occurs. Because the cross section into this

TABLE 1

CONTINUOUS ABSORPTION CROSS SECTION PER OH MOLECULE (cm^2)

eV	1000K	2000K	3000K	4000K	5000K	6000K	7000K	8000K	9000K
2.0	0.00-00	5.66-32	4.29-29	1.10-27	7.35-27	2.52-26	5.92-26	1.10-25	1.76-25
2.2	0.00-00	3.20-31	2.43-28	6.23-27	4.16-26	1.42-25	3.35-25	6.23-25	9.95-25
2.4	0.00-00	1.42-30	1.06-27	2.72-26	1.81-25	6.21-25	1.46-24	2.71-24	4.33-24
2.6	0.00-00	4.93-30	3.67-27	9.36-26	6.23-25	2.13-24	5.01-24	9.32-24	1.49-23
2.8	1.63-36	1.51-29	1.05-26	2.66-25	1.77-24	6.05-24	1.42-23	2.64-23	4.21-23
3.0	3.24-35	5.30-29	2.67-26	6.51-25	4.28-24	1.46-23	3.41-23	6.34-23	1.01-22
3.2	2.25-34	2.01-28	6.25-26	1.41-24	9.05-24	3.05-23	7.11-23	1.32-22	2.09-22
3.4	1.20-33	7.95-28	1.48-25	2.86-24	1.75-23	5.79-23	1.33-22	2.45-22	3.88-22
3.6	5.71-33	2.94-27	3.71-25	5.78-24	3.25-23	1.03-22	2.33-22	4.23-22	6.64-22
3.8	9.83-31	1.13-26	9.61-25	1.19-23	5.98-23	1.79-22	3.89-22	6.92-22	1.07-21
4.0	8.08-30	4.25-26	2.49-24	2.54-23	1.12-22	3.11-22	6.45-22	1.11-21	1.68-21
4.2	5.06-29	1.66-25	6.47-24	5.48-23	2.15-22	5.51-22	1.08-21	1.80-21	2.64-21
4.4	4.98-28	6.56-25	1.68-23	1.18-22	4.16-22	9.89-22	1.85-21	2.94-21	4.21-21
4.6	1.31-26	2.90-24	4.57-23	2.56-22	8.02-22	1.77-21	3.15-21	4.84-21	6.73-21
4.8	8.98-26	1.16-23	1.26-22	5.62-22	1.55-21	3.16-21	5.33-21	7.90-21	1.07-20
5.0	6.48-25	4.60-23	3.54-22	1.26-21	3.02-21	5.66-21	9.00-21	1.28-20	1.68-20
5.2	3.62-24	1.71-22	9.74-22	2.86-21	5.98-21	1.02-20	1.53-20	2.07-20	2.64-20
5.4	1.88-23	5.85-22	2.60-21	6.42-21	1.19-20	1.86-20	2.60-20	3.37-20	4.13-20
5.6	8.48-23	1.81-21	6.58-21	1.40-20	2.33-20	3.36-20	4.43-20	5.48-20	6.48-20
5.8	3.53-22	5.05-21	1.56-20	2.93-20	4.45-20	5.98-20	7.46-20	8.84-20	1.01-19
6.0	1.32-21	1.28-20	3.41-20	5.81-20	8.15-20	1.03-19	1.23-19	1.40-19	1.55-19
6.1	2.50-21	1.97-20	4.91-20	7.98-20	1.08-19	1.33-19	1.55-19	1.74-19	1.90-19
6.2	4.66-21	2.97-20	6.91-20	1.08-19	1.41-19	1.70-19	1.93-19	2.14-19	2.31-19
6.3	8.53-21	4.40-20	9.52-20	1.42-19	1.81-19	2.12-19	2.38-19	2.59-19	2.77-19
6.4	1.54-20	6.38-20	1.28-19	1.84-19	2.27-19	2.61-19	2.88-19	3.10-19	3.27-19
6.5	2.72-20	9.09-20	1.69-19	2.32-19	2.80-19	3.16-19	3.43-19	3.64-19	3.81-19
6.6	4.74-20	1.28-19	2.18-19	2.87-19	3.37-19	3.73-19	4.00-19	4.21-19	4.37-19
6.7	8.12-20	1.77-19	2.76-19	3.48-19	3.98-19	4.33-19	4.59-19	4.79-19	4.94-19
6.8	1.36-19	2.45-19	3.47-19	4.16-19	4.63-19	4.96-19	5.20-19	5.39-19	5.53-19
6.9	2.23-19	3.38-19	4.34-19	4.97-19	5.38-19	5.67-19	5.88-19	6.04-19	6.17-19
7.0	3.56-19	4.68-19	5.49-19	5.98-19	6.30-19	6.53-19	6.70-19	6.83-19	6.94-19
7.1	5.48-19	6.46-19	7.02-19	7.32-19	7.51-19	7.66-19	7.78-19	7.87-19	7.95-19
7.2	8.10-19	8.82-19	9.05-19	9.11-19	9.15-19	9.19-19	9.23-19	9.26-19	9.28-19
7.3	1.14-18	1.18-18	1.16-18	1.14-18	1.13-18	1.12-18	1.11-18	1.10-18	1.10-18
7.4	1.53-18	1.52-18	1.46-18	1.41-18	1.38-18	1.35-18	1.33-18	1.32-18	1.30-18
7.5	1.94-18	1.89-18	1.79-18	1.71-18	1.65-18	1.61-18	1.57-18	1.54-18	1.52-18
7.6	2.34-18	2.23-18	2.10-18	1.99-18	1.92-18	1.85-18	1.80-18	1.76-18	1.72-18
7.7	2.65-18	2.51-18	2.35-18	2.22-18	2.13-18	2.05-18	1.99-18	1.93-18	1.88-18
7.8	2.85-18	2.68-18	2.50-18	2.37-18	2.26-18	2.18-18	2.10-18	2.04-18	1.98-18
7.9	2.91-18	2.72-18	2.54-18	2.41-18	2.30-18	2.21-18	2.13-18	2.06-18	2.00-18
8.0	2.82-18	2.63-18	2.47-18	2.34-18	2.24-18	2.15-18	2.08-18	2.01-18	1.95-18
8.1	2.60-18	2.44-18	2.30-18	2.19-18	2.10-18	2.02-18	1.96-18	1.89-18	1.83-18
8.2	2.31-18	2.17-18	2.06-18	1.98-18	1.91-18	1.85-18	1.79-18	1.73-18	1.68-18
8.3	1.98-18	1.87-18	1.80-18	1.74-18	1.69-18	1.64-18	1.60-18	1.55-18	1.51-18
8.4	1.64-18	1.58-18	1.54-18	1.50-18	1.47-18	1.44-18	1.41-18	1.38-18	1.35-18
8.5	1.34-18	1.31-18	1.30-18	1.28-18	1.27-18	1.25-18	1.23-18	1.22-18	1.20-18
8.6	1.09-18	1.08-18	1.09-18	1.10-18	1.10-18	1.10-18	1.09-18	1.08-18	1.07-18
8.7	9.03-19	9.12-19	9.39-19	9.58-19	9.70-19	9.76-19	9.79-19	9.80-19	9.78-19
8.8	7.82-19	8.01-19	8.35-19	8.62-19	8.82-19	8.96-19	9.07-19	9.15-19	9.20-19
8.9	7.27-19	7.50-19	7.85-19	8.15-19	8.40-19	8.61-19	8.77-19	8.90-19	9.00-19
9.0	7.37-19	7.58-19	7.89-19	8.19-19	8.47-19	8.71-19	8.91-19	9.07-19	9.20-19
9.1	8.11-19	8.25-19	8.49-19	8.77-19	9.04-19	9.30-19	9.52-19	9.69-19	9.83-19
9.2	9.38-19	9.44-19	9.61-19	9.86-19	1.01-18	1.04-18	1.06-18	1.08-18	1.09-18
9.3	1.10-18	1.10-18	1.12-18	1.14-18	1.16-18	1.19-18	1.21-18	1.22-18	1.23-18
9.4	1.29-18	1.29-18	1.30-18	1.32-18	1.35-18	1.37-18	1.38-18	1.39-18	1.40-18
9.5	1.48-18	1.48-18	1.49-18	1.52-18	1.54-18	1.56-18	1.57-18	1.57-18	1.57-18
9.6	1.63-18	1.64-18	1.67-18	1.70-18	1.73-18	1.74-18	1.75-18	1.75-18	1.74-18
9.7	1.73-18	1.77-18	1.82-18	1.86-18	1.89-18	1.90-18	1.91-18	1.90-18	1.89-18
9.8	1.79-18	1.85-18	1.92-18	1.98-18	2.01-18	2.03-18	2.03-18	2.02-18	2.01-18
9.9	1.79-18	1.89-18	2.00-18	2.07-18	2.11-18	2.12-18	2.13-18	2.12-18	2.10-18
10.0	1.79-18	1.92-18	2.05-18	2.13-18	2.17-18	2.19-18	2.19-18	2.18-18	2.16-18
10.1	1.77-18	1.94-18	2.09-18	2.18-18	2.23-18	2.24-18	2.24-18	2.23-18	2.21-18
10.2	1.78-18	1.97-18	2.13-18	2.23-18	2.27-18	2.29-18	2.29-18	2.28-18	2.25-18
10.3	1.84-18	2.04-18	2.20-18	2.29-18	2.33-18	2.35-18	2.34-18	2.32-18	2.30-18
10.4	1.95-18	2.15-18	2.31-18	2.38-18	2.41-18	2.42-18	2.40-18	2.38-18	2.35-18
10.5	2.12-18	2.32-18	2.45-18	2.50-18	2.52-18	2.51-18	2.49-18	2.46-18	2.43-18
10.6	2.35-18	2.54-18	2.63-18	2.66-18	2.65-18	2.63-18	2.60-18	2.56-18	2.52-18
10.7	2.66-18	2.82-18	2.87-18	2.86-18	2.83-18	2.79-18	2.74-18	2.69-18	2.65-18
10.8	3.05-18	3.16-18	3.15-18	3.10-18	3.04-18	2.98-18	2.92-18	2.86-18	2.80-18
10.9	3.50-18	3.56-18	3.49-18	3.39-18	3.30-18	3.21-18	3.13-18	3.06-18	2.99-18
11.0	4.02-18	4.01-18	3.88-18	3.73-18	3.60-18	3.49-18	3.39-18	3.30-18	3.22-18
11.1	4.61-18	4.52-18	4.31-18	4.11-18	3.94-18	3.80-18	3.68-18	3.58-18	3.48-18
11.2	5.24-18	5.07-18	4.78-18	4.52-18	4.32-18	4.15-18	4.01-18	3.89-18	3.77-18
11.3	5.89-18	5.64-18	5.27-18	4.96-18	4.72-18	4.53-18	4.36-18	4.22-18	4.09-18
11.4	6.52-18	6.18-18	5.74-18	5.39-18	5.12-18	4.90-18	4.71-18	4.54-18	4.39-18
11.5	7.08-18	6.66-18	6.16-18	5.77-18	5.47-18	5.22-18	5.02-18	4.83-18	4.66-18
11.6	7.49-18	7.01-18	6.48-18	6.06-18	5.73-18	5.47-18	5.24-18	5.04-18	4.86-18
11.7	7.72-18	7.19-18	6.63-18	6.20-18	5.87-18	5.59-18	5.35-18	5.14-18	4.95-18
11.8	7.70-18	7.14-18	6.59-18	6.17-18	5.84-18	5.56-18	5.32-18	5.11-18	4.91-18
11.9	7.43-18	6.88-18	6.36-18	5.96-18	5.64-18	5.37-18	5.14-18	4.93-18	4.73-18
12.0	6.92-18	6.41-18	5.93-18	5.57-18	5.28-18	5.03-18	4.81-18	4.61-18	4.43-18
12.1	6.23-18	5.77-18	5.36-18	5.05-18	4.79-18	4.57-18	4.37-18	4.19-18	4.02-18
12.2	5.42-18	5.03-18	4.69-18	4.43-18	4.21-18	4.02-18	3.85-18	3.69-18	3.54-18
12.3	4.56-18	4.23-18	3.97-18	3.76-18	3.58-18	3.42-18	3.28-18	3.14-18	3.02-18
12.4	3.71-18	3.45-18	3.24-18	3.08-18	2.94-18	2.82-18	2.70-18	2.59-18	2.49-18
12.5	2.90-18	2.71-18	2.56-18	2.44-18	2.33-18	2.24-18	2.14-18	2.06-18	1.98-18
12.6	2.19-18	2.05-18	1.94-18	1.85-18	1.78-18	1.71-18	1.64-18	1.57-18	1.51-18
12.7	1.59-18	1.48-18	1.41-18	1.35-18	1.30-18	1.25-18	1.20-18	1.15-18	1.11-18
12.8	1.10-18	1.03-18	9.78-19	9.39-19	9.02-19	8.68-19	8.34-19	8.02-19	7.72-19
12.9	7.23-19	6.74-19	6.42-19	6.17-19	5.93-19	5.71-19	5.49-19	5.29-19	5.09-19
13.0	4.47-19	4.16-19	3.95-19	3.79-19	3.64-19	3.51-19	3.38-19	3.26-19	3.14-19
13.1	2.57-19	2.37-19	2.24-19	2.14-19	2.06-19	1.98-19	1.91-19	1.84-19	1.78-19
13.2	1.35-19	1.23-19	1.14-19	1.08-19	1.04-19	9.99-20	9.64-20	9.32-20	9.01-20
13.3	6.22-20	5.50-20	4.98-20	4.64-20	4.42-20	4.25-20	4.11-20	3.98-20	3.86-20
13.4	2.35-20	1.98-20	1.69-20	1.53-20	1.43-20	1.37-20	1.33-20	1.30-20	1.27-20
13.5	5.69-21	4.58-21	3.76-21	3.34-21	3.15-21	3.07-21	3.03-21	3.01-21	2.99-21
13.6	1.00-21	8.86-22	8.08-22	7.69-22	7.53-22	7.48-22	7.44-22	7.40-22	7.33-22
13.7	7.68-22	6.71-22	5.89-22	5.27-22	4.79-22	4.39-22	4.06-22	3.77-22	3.52-22
13.8	5.97-22	5.19-22	4.51-22	4.03-22	3.68-22	3.40-22	3.18-22	2.99-22	2.83-22
13.9	4.61-22	4.02-22	3.47-22	3.09-22	2.81-22	2.60-22	2.43-22	2.29-22	2.17-22
14.0	3.47-22	3.05-22	2.63-22	2.32-22	2.10-22	1.94-22	1.81-22	1.71-22	1.62-22
14.1	2.49-22	2.23-22	1.95-22	1.73-22	1.57-22	1.46-22	1.37-22	1.30-22	1.23-22
14.2	1.64-22	1.55-22	1.40-22	1.28-22	1.19-22	1.12-22	1.07-22	1.03-22	9.86-23
14.3	9.53-23	9.79-23	9.42-23	8.95-23	8.58-23	8.30-23	8.06-23	7.85-23	7.65-23
14.4	3.09-23	4.44-23	5.06-23	5.30-23	5.42-23	5.50-23	5.53-23	5.53-23	5.51-23
14.5	5.21-24	1.97-23	2.81-23	3.25-23	3.54-23	3.74-23	3.89-23	3.98-23	4.03-23
14.6	3.42-24	1.29-23	1.86-23	2.19-23	2.44-23	2.64-23	2.79-23	2.89-23	2.96-23
14.7	1.62-24	6.15-24	9.10-24	1.14-23	1.34-23	1.53-23	1.68-23	1.81-23	1.90-23
14.8	2.48-29	4.88-26	5.62-25	1.79-24	3.44-24	5.15-24	6.71-24	8.03-24	9.09-24
14.9	2.05-29	4.03-26	4.65-25	1.48-24	2.85-24	4.26-24	5.54-24	6.63-24	7.52-24
15.0	1.88-29	3.71-26	4.28-25	1.36-24	2.62-24	3.92-24	5.11-24	6.11-24	6.92-24

1987ApJ...322..992K

TABLE 2

CONTINUOUS ABSORPTION CROSS SECTION PER CH MOLECULE (cm^2)

eV	1000K	2000K	3000K	4000K	5000K	6000K	7000K	8000K	9000K
0.2	0.00-00	1.87-33	7.36-31	1.19-29	5.53-29	1.42-28	2.63-28	4.03-28	5.49-28
0.3	0.00-00	2.58-32	1.02-29	1.65-28	7.68-28	1.97-27	3.66-27	5.61-27	7.63-27
0.4	0.00-00	3.92-31	1.55-28	2.50-27	1.17-26	3.00-26	5.56-26	8.53-26	1.16-25
0.5	0.00-00	3.07-30	1.20-27	1.94-26	9.05-26	2.32-25	4.30-25	6.59-25	8.98-25
0.6	4.71-38	1.23-29	4.71-27	7.54-26	3.49-25	8.93-25	1.65-24	2.53-24	3.44-24
0.7	1.56-37	3.04-29	1.11-26	1.74-25	7.97-25	2.02-24	3.73-24	5.69-24	7.71-24
0.8	6.06-37	6.13-29	2.09-26	3.18-25	1.44-24	3.61-24	6.60-24	1.00-23	1.35-23
0.9	1.74-36	1.14-28	3.58-26	5.24-25	2.32-24	5.74-24	1.04-23	1.57-23	2.10-23
1.0	4.26-36	1.97-28	5.75-26	8.16-25	3.54-24	8.66-24	1.55-23	2.33-23	3.11-23
1.1	1.44-35	3.35-28	9.05-26	1.25-24	5.31-24	1.28-23	2.29-23	3.41-23	4.54-23
1.2	7.40-35	6.01-28	1.43-25	1.89-24	7.90-24	1.89-23	3.34-23	4.94-23	6.55-23
1.3	5.62-34	1.37-27	2.47-25	3.00-24	1.20-23	2.82-23	4.91-23	7.20-23	9.48-23
1.4	1.52-33	2.06-27	3.49-25	4.15-24	1.65-23	3.82-23	6.63-23	9.69-23	1.27-22
1.5	1.93-32	8.23-27	7.85-25	7.58-24	2.75-23	6.07-23	1.02-22	1.46-22	1.89-22
1.6	3.61-32	1.25-26	1.16-24	1.09-23	3.85-23	8.39-23	1.40-22	1.98-22	2.55-22
1.7	5.81-31	6.10-26	3.09-24	2.21-23	6.88-23	1.40-22	2.22-22	3.07-22	3.87-22
1.8	1.52-30	1.22-25	5.20-24	3.35-23	9.84-23	1.93-22	3.01-22	4.09-22	5.10-22
1.9	1.23-29	3.03-25	9.15-24	5.24-23	1.47-22	2.81-22	4.31-22	5.81-22	7.20-22
2.0	3.80-29	8.19-25	2.24-23	1.13-22	2.84-22	5.06-22	7.39-22	9.60-22	1.16-21
2.1	8.19-29	1.41-24	3.37-23	1.57-22	3.78-22	6.57-22	9.47-22	1.22-21	1.46-21
2.2	1.87-27	7.31-24	1.01-22	3.63-22	7.63-22	1.22-21	1.68-21	2.09-21	2.45-21
2.3	1.07-27	6.33-24	1.18-22	4.86-22	1.07-21	1.75-21	2.39-21	2.96-21	3.44-21
2.4	7.52-27	2.01-23	2.60-22	8.48-22	1.62-21	2.39-21	3.06-21	3.61-21	4.06-21
2.5	9.00-26	7.60-23	6.40-22	1.73-21	3.04-21	4.30-21	5.39-21	6.30-21	7.04-21
2.6	3.23-25	1.40-22	1.17-21	3.27-21	5.82-21	8.24-21	1.03-20	1.19-20	1.32-20
2.7	3.84-24	7.47-22	4.15-21	9.03-21	1.36-20	1.70-20	1.95-20	2.12-20	2.23-20
2.8	6.77-23	3.15-21	1.20-20	2.20-20	3.02-20	3.58-20	3.95-20	4.18-20	4.31-20
2.9	3.06-22	9.34-21	2.95-20	4.91-20	6.32-20	7.21-20	7.73-20	8.01-20	8.16-20
3.0	1.17-21	2.29-20	6.47-20	1.01-19	1.24-19	1.37-19	1.43-19	1.46-19	1.46-19
3.1	4.35-21	4.65-20	1.15-19	1.70-19	2.02-19	2.18-19	2.24-19	2.24-19	2.22-19
3.2	1.38-20	8.51-20	1.75-19	2.40-19	2.74-19	2.88-19	2.91-19	2.89-19	2.84-19
3.3	3.26-20	1.41-19	2.42-19	3.01-19	3.28-19	3.35-19	3.32-19	3.26-19	3.17-19
3.4	5.86-20	1.96-19	2.93-19	3.38-19	3.52-19	3.49-19	3.40-19	3.29-19	3.18-19
3.5	8.86-20	2.21-19	2.99-19	3.28-19	3.30-19	3.21-19	3.09-19	2.97-19	2.86-19
3.6	1.22-19	2.14-19	2.62-19	2.75-19	2.71-19	2.61-19	2.50-19	2.41-19	2.32-19
3.7	1.46-19	1.87-19	2.06-19	2.07-19	2.00-19	1.93-19	1.86-19	1.80-19	1.75-19
3.8	1.37-19	1.45-19	1.46-19	1.42-19	1.37-19	1.32-19	1.29-19	1.27-19	1.26-19
3.9	9.56-20	9.25-20	8.93-20	8.63-20	8.49-20	8.51-20	8.62-20	8.75-20	8.89-20
4.0	4.46-20	4.25-20	4.15-20	4.24-20	4.56-20	5.01-20	5.49-20	5.93-20	6.32-20
4.1	1.72-20	1.66-20	1.73-20	2.06-20	2.67-20	3.42-20	4.18-20	4.86-20	5.44-20
4.2	7.18-21	7.06-21	8.19-21	1.23-20	1.93-20	2.76-20	3.58-20	4.32-20	4.94-20
4.3	2.93-21	2.99-21	4.87-21	1.07-20	1.97-20	2.96-20	3.88-20	4.67-20	5.32-20
4.4	1.18-21	1.35-21	4.31-21	1.28-20	2.49-20	3.75-20	4.87-20	5.80-20	6.55-20
4.5	3.91-22	6.63-22	4.17-21	1.39-20	2.78-20	4.22-20	5.50-20	6.55-20	7.39-20
4.6	6.47-23	6.81-22	6.22-21	1.91-20	3.57-20	5.21-20	6.61-20	7.72-20	8.59-20
4.7	5.63-24	1.21-21	1.06-20	2.91-20	5.03-20	6.93-20	8.45-20	9.60-20	1.04-19
4.8	3.99-24	1.77-21	1.42-20	3.74-20	6.27-20	8.46-20	1.02-19	1.14-19	1.23-19
4.9	1.85-23	3.50-21	2.11-20	4.98-20	7.98-20	1.05-19	1.25-19	1.39-19	1.49-19
5.0	4.99-23	7.02-21	3.46-20	7.32-20	1.10-19	1.39-19	1.60-19	1.74-19	1.84-19
5.1	1.18-22	1.15-20	5.15-20	1.02-19	1.45-19	1.77-19	1.99-19	2.13-19	2.22-19
5.2	5.18-22	2.20-20	7.88-20	1.40-19	1.89-19	2.22-19	2.43-19	2.56-19	2.64-19
5.3	1.50-21	4.09-20	1.17-19	1.88-19	2.40-19	2.74-19	2.96-19	3.09-19	3.17-19
5.4	3.28-21	6.30-20	1.61-19	2.45-19	3.05-19	3.45-19	3.69-19	3.84-19	3.92-19
5.5	1.23-20	1.19-19	2.58-19	3.64-19	4.31-19	4.69-19	4.89-19	4.97-19	4.98-19
5.6	3.92-20	2.43-19	4.36-19	5.52-19	6.09-19	6.28-19	6.28-19	6.19-19	6.06-19
5.7	8.26-20	3.81-19	6.00-19	7.04-19	7.37-19	7.36-19	7.19-19	6.97-19	6.74-19
5.8	1.43-19	5.06-19	7.11-19	7.92-19	8.10-19	8.02-19	7.82-19	7.59-19	7.37-19
5.9	6.92-19	9.54-19	1.05-18	1.08-18	1.07-18	1.05-18	1.03-18	1.00-18	9.75-19
6.0	1.72-18	2.02-18	2.06-18	2.00-18	1.91-18	1.82-18	1.73-18	1.66-18	1.59-18
6.1	4.12-18	4.23-18	3.98-18	3.63-18	3.29-18	3.00-18	2.76-18	2.57-18	2.42-18
6.2	7.53-18	6.78-18	5.89-18	5.10-18	4.45-18	3.95-18	3.56-18	3.25-18	3.02-18
6.3	8.05-18	7.06-18	6.06-18	5.22-18	4.55-18	4.03-18	3.63-18	3.31-18	3.07-18
6.4	6.72-18	5.89-18	5.12-18	4.49-18	3.98-18	3.57-18	3.24-18	2.99-18	2.78-18
6.5	4.72-18	4.18-18	3.75-18	3.42-18	3.12-18	2.88-18	2.67-18	2.50-18	2.36-18
6.6	2.76-18	2.53-18	2.46-18	2.42-18	2.35-18	2.27-18	2.18-18	2.10-18	2.02-18
6.7	1.43-18	1.42-18	1.60-18	1.78-18	1.89-18	1.92-18	1.92-18	1.90-18	1.86-18
6.8	7.06-19	8.16-19	1.14-18	1.46-18	1.67-18	1.79-18	1.84-18	1.85-18	1.84-18
6.9	3.27-19	5.03-19	9.17-19	1.32-18	1.59-18	1.75-18	1.83-18	1.86-18	1.87-18
7.0	1.48-19	3.63-19	8.01-19	1.22-18	1.51-18	1.69-18	1.79-18	1.85-18	1.87-18
7.1	8.52-20	3.36-19	7.74-19	1.19-18	1.49-18	1.69-18	1.82-18	1.90-18	1.94-18
7.2	9.05-20	4.11-19	8.86-19	1.32-18	1.65-18	1.87-18	2.00-18	2.08-18	2.13-18
7.3	1.61-19	6.90-19	1.34-18	1.83-18	2.15-18	2.32-18	2.40-18	2.43-18	2.43-18
7.4	3.45-19	1.24-18	2.04-18	2.49-18	2.68-18	2.72-18	2.68-18	2.62-18	2.55-18
7.5	7.61-19	2.09-18	2.89-18	3.12-18	3.08-18	2.95-18	2.79-18	2.64-18	2.51-18
7.6	1.48-18	2.25-18	2.60-18	2.67-18	2.62-18	2.53-18	2.43-18	2.34-18	2.26-18
7.7	4.25-18	5.01-18	5.12-18	4.94-18	4.65-18	4.35-18	4.08-18	3.85-18	3.65-18
7.8	1.60-17	1.64-17	1.50-17	1.31-17	1.14-17	9.94-18	8.80-18	7.92-18	7.22-18
7.9	3.82-17	3.24-17	2.64-17	2.14-17	1.76-17	1.48-17	1.27-17	1.12-17	9.99-18
8.0	2.24-17	2.02-17	1.75-17	1.50-17	1.29-17	1.13-17	9.96-18	8.95-18	8.17-18
8.1	1.21-17	1.16-17	1.07-17	9.64-18	8.63-18	7.75-18	7.04-18	6.46-18	6.00-18
8.2	6.46-18	6.31-18	6.02-18	5.61-18	5.17-18	4.77-18	4.42-18	4.13-18	3.90-18
8.3	2.45-18	2.53-18	2.58-18	2.55-18	2.47-18	2.37-18	2.27-18	2.18-18	2.10-18
8.4	6.04-19	6.82-19	7.83-19	8.55-19	8.98-19	9.17-19	9.22-19	9.20-19	9.13-19
8.5	7.77-20	9.99-20	1.45-19	1.93-19	2.33-19	2.64-19	2.85-19	3.00-19	3.11-19
8.6	4.13-22	4.86-21	1.76-20	3.38-20	4.91-20	6.19-20	7.19-20	7.96-20	8.54-20
8.7	3.94-21	1.77-20	3.02-20	3.78-20	4.15-20	4.30-20	4.33-20	4.31-20	4.26-20
8.8	5.08-21	2.63-20	4.60-20	5.75-20	6.21-20	6.27-20	6.13-20	5.92-20	5.69-20
8.9	3.16-21	2.06-20	4.08-20	5.52-20	6.33-20	6.69-20	6.79-20	6.75-20	6.65-20
9.0	1.17-21	1.05-20	2.48-20	3.76-20	4.68-20	5.27-20	5.62-20	5.82-20	5.93-20
9.1	2.76-22	3.59-21	1.10-20	1.95-20	2.67-20	3.22-20	3.61-20	3.89-20	4.09-20
9.2	2.68-23	1.05-21	4.06-21	7.76-21	1.12-20	1.43-20	1.68-20	1.89-20	2.06-20
9.3	5.01-24	3.94-22	1.69-21	3.46-21	5.32-21	7.12-21	8.76-21	1.02-20	1.14-20
9.4	8.53-24	4.91-22	1.77-21	3.20-21	4.49-21	5.60-21	6.54-21	7.32-21	7.98-21
9.5	1.27-23	6.02-22	1.96-21	3.31-21	4.35-21	5.10-21	5.64-21	6.02-21	6.30-21
9.6	6.03-24	3.63-22	1.33-21	2.38-21	3.24-21	3.86-21	4.29-21	4.57-21	4.76-21
9.7	2.91-24	2.15-22	8.48-22	1.60-21	2.24-21	2.72-21	3.06-21	3.30-21	3.46-21
9.8	1.54-24	1.19-22	4.83-22	9.32-22	1.34-21	1.65-21	1.89-21	2.05-21	2.17-21
9.9	5.71-25	4.80-23	2.06-22	4.17-22	6.22-22	7.96-22	9.32-22	1.03-21	1.11-21
10.0	1.04-25	1.07-23	5.15-23	1.13-22	1.81-22	2.42-22	2.93-22	3.33-22	3.64-22
10.1	4.70-27	9.97-25	6.32-24	1.69-23	3.05-23	4.42-23	5.62-23	6.61-23	7.40-23
10.2	2.75-27	5.85-25	3.33-24	7.44-24	1.14-23	1.45-23	1.68-23	1.84-23	1.95-23
10.3	8.75-29	2.82-25	3.01-24	8.05-24	1.28-23	1.60-23	1.78-23	1.86-23	1.88-23
10.4	1.55-28	5.00-25	5.33-24	1.42-23	2.25-23	2.81-23	3.11-23	3.25-23	3.28-23
10.5	9.40-29	3.03-25	3.23-24	8.60-24	1.36-23	1.70-23	1.89-23	1.97-23	1.98-23

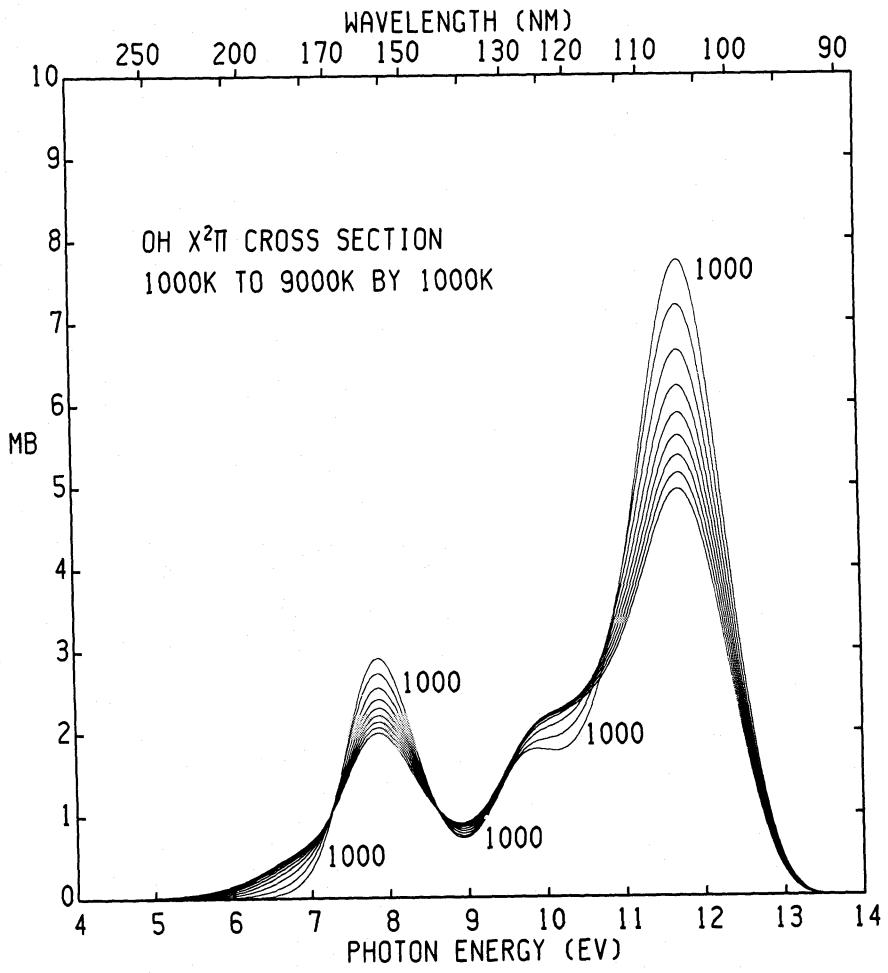

FIG. 2

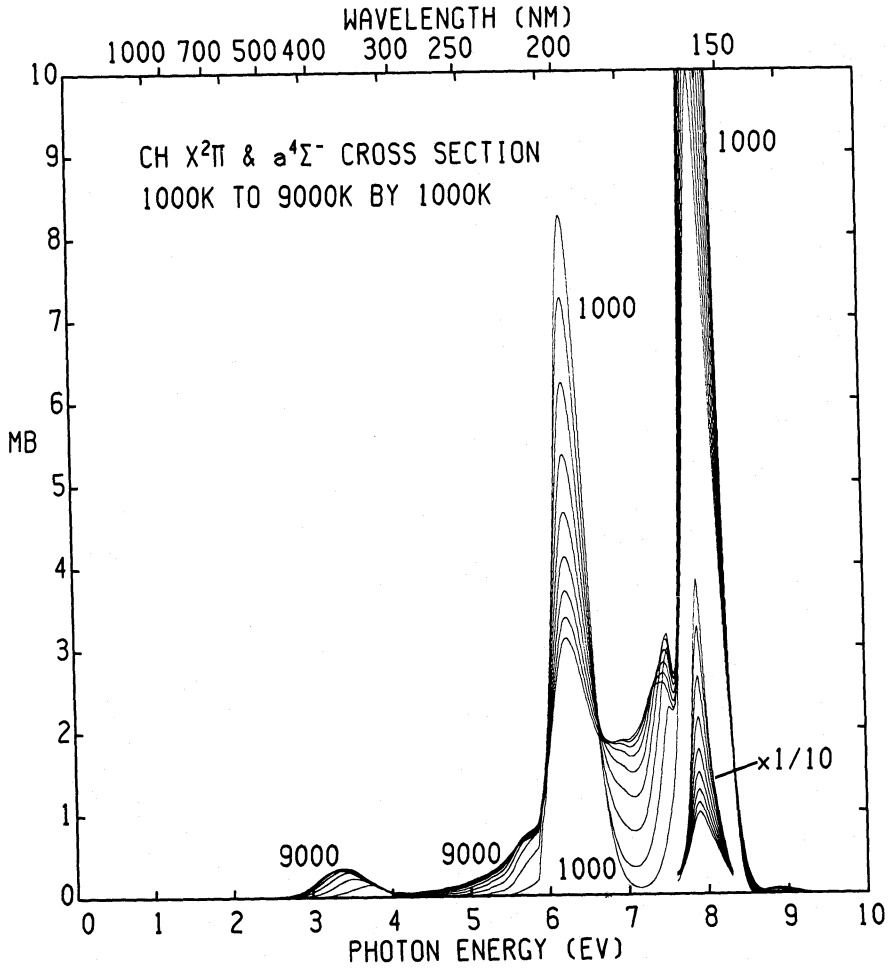

FIG. 3

FIG. 2.—LTE Boltzmann-averaged cross sections per OH molecule as functions of photon energy (*lower scale*) or wavelength (*upper scale*). The cross sections are plotted for temperatures ranging from 1000 K to 9000 K, in steps of 1000 K.

FIG. 3.—As Fig. 2, but for CH

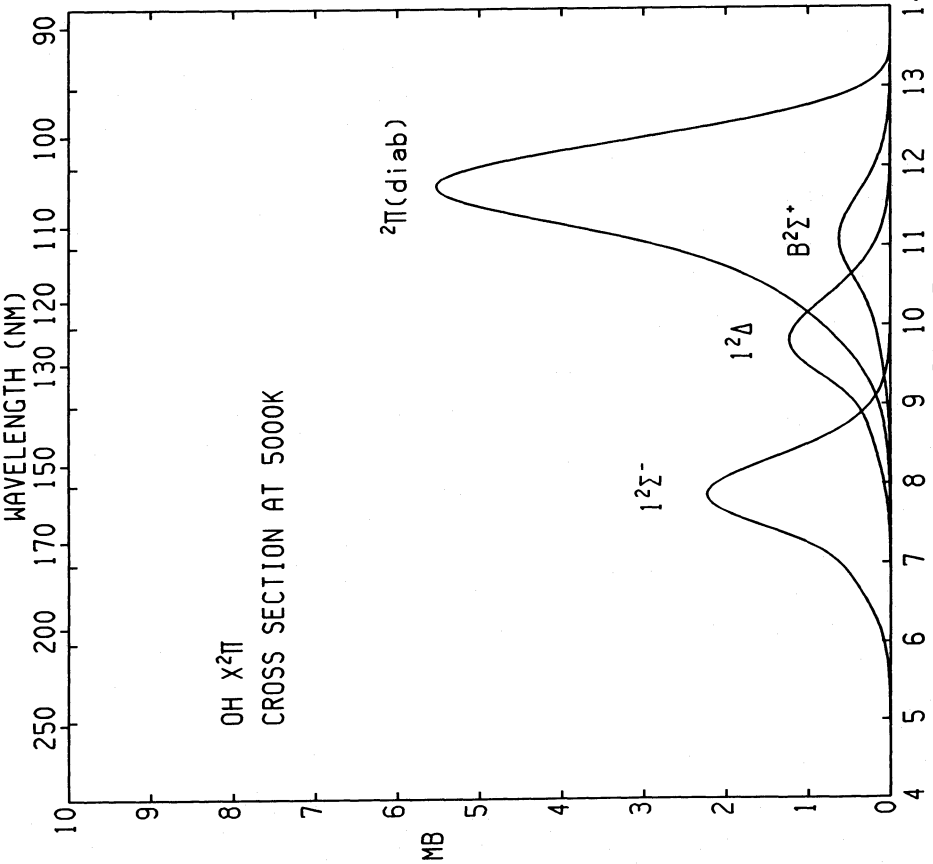

FIG. 4

FIG. 4.—Contribution of the individual electronic transitions in OH to the total LTE Boltzmann-averaged cross sections at 5000 K as functions of photon energy (*lower scale*) to wavelength (*upper scale*).

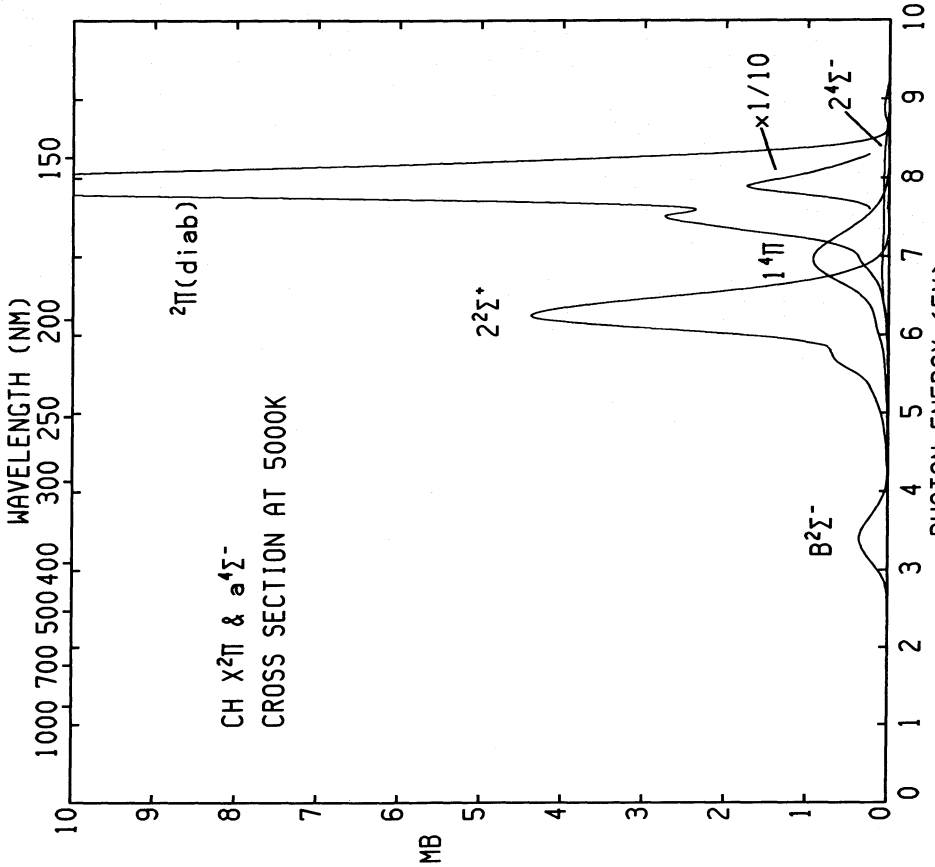

FIG. 5

FIG. 5.—As Fig. 4, but for CH

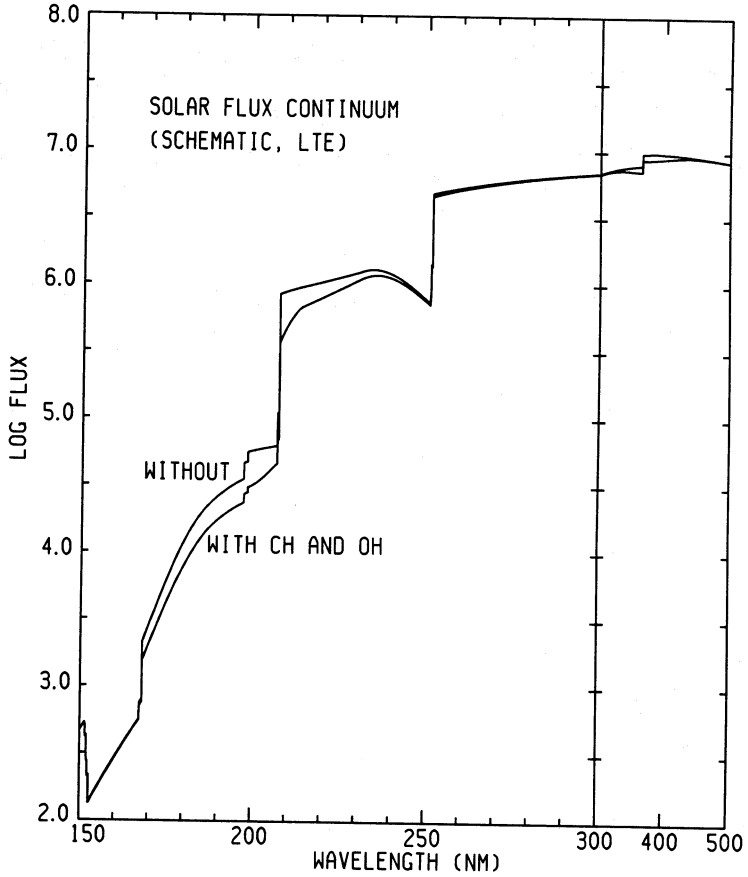

FIG. 6.—Solar ultraviolet continuum flux H_λ (in ergs cm^{-2} s^{-1} sr^{-1} nm^{-1}) computed with and without inclusion of OH and CH continuous absorption

state is not well determined, the actual contribution is uncertain by a factor of about 2. Neither CH nor OH appears to have significant opacity between 250 and 300 nm. When line opacity is included in the models, the relative effect of the OH and CH continuous absorption on the actual flux is much less. It will be very small in the cores of strong lines, but still remains relatively important in the regions between lines.

The effects of the OH and CH continuous opacity should be much stronger in cooler stars, where the abundance of these molecules is significantly larger than in the Sun. Because of the importance of the CH $B^2\Sigma^-$ channel around 400 nm, better determinations of the $B^2\Sigma^-$ potential and the $B^2\Sigma^- - X^2\Pi$ cross sections are warranted. Further spectroscopic investigations of the CH $a^4\Sigma^-$ state are also needed. It will be important to investigate whether continuous absorptions of other abundant molecules such as H_2O, NH, SH, and HCl can contribute significantly to the opacity in these cool stars as well.

This work is supported in part (for R. L. K.) by NASA grant NSG-7054 and by NSF grant AST-85189900 of computer time at the San Diego Supercomputer Center. E. v.D. acknowledges the hospitality of the Institute for Advanced Study in Princeton and its support through NSF grant PHY-8217352.

REFERENCES

Allen, R. G. 1978, Ph.D. thesis, University of Arizona.
Coxon, J. A., and Foster, S. C. 1982, *Canadian J. Phys.*, **60**, 41.
Fox, P. W., and Tarafdar, S. P. 1978, *Solar Phys.*, **60**, 241.
Kurucz, R. L., and Avrett, E. H. 1981, *Smithsonian Ap. Obs. Spec. Rep.*, No. 391.
Tarafdar, S. P., and Das, P. K. 1975, *M.N.R.A.S.*, **170**, 559.
van Dishoeck, E. F. 1987, *J. Chem. Phys.*, **86**, 196.
van Dishoeck, E. F., and Dalgarno, A. 1983, *J. Chem. Phys.*, **79**, 873.
———. 1984, *Ap. J.*, **277**, 576.
van Dishoeck, E. F., Langhoff, S. R., and Dalgarno, A. 1983, *J. Chem. Phys.*, **78**, 4552.
van Dishoeck, E. F., van Hemert, M. C., Allison, A. C., and Dalgarno, A. 1984, *J. Chem. Phys.*, **81**, 5709.

ROBERT L. KURUCZ and EWINE F. VAN DISHOECK: Center for Astrophysics, 60 Garden Street, Cambridge MA 01238

S. P. TARAFDAR: Tata Institute of Fundamental Research, Homi Bhabha Road, Bombay 400 005, India